Supplementary Materials
Molecular Biology of the Cell
Mercadante *et al*.

Supplemental Material

Table Captions

Table S1: Parameters. All parameter values without reference are approximated to match biological results.

Figure Captions

Figure S1: Graphical representation and validation of experimental conditions used in Figures 1, 2, and 3. (A) Representative NuMA cortical enrichment ratios calculated as peak intensity at the cortex/peak intensity within the cytoplasm along a radius that extends through individual spindle poles. (B) Quantification of the fraction of mitotic cells exhibiting each pattern of NuMA enrichment ratios represented in panel (A). (C) Representative fixed-cell images of NuMA and dynein (p150) staining in the control (siScr), as well as in the Afadin and LGN depleted cells (siLGN and siAfadin, respectively). (D,E,F) Overview of the experimental timeline for induction of centrosome amplification and disruption of cortical dynein localization in cell culture. (D,E, left) Depiction of the experimental timelines to induce siRNA-based depletion of Afadin or LGN in mitotic RPE cells concurrently induced to have centrosome amplification through either overexpression of PLK4 (D) or dihydrocytochalasin B (DCB)-induced cytokinesis failure (E). (D,middle) Quantification of the number of centrioles in the indPLK4 cells. (D,E, right) Relative expression of Afadin (siAfa) or LGN (siLGN) following indicated duration of siRNA-mediated depletion of Afadin and LGN. (F) Timeline (left) with quantification of centrosome number (middle) and relative expression of Afadin (siAfa) or LGN (siLGN) after 72 h or 48 h, respectively, of siRNA-mediated depletion in MDA-MB-231 cancer cells (right). Controls are denoted by siCtl in (D,E,F). Significance determined by student's t-test; ***$p < 0.001$, ****$p < 0.0001$.

Figure S2: Microtubule dynamics and motor-derived forces are dependent on probabilities of binding and/or distances between microtubule and motor. (A) Schematic of the mitotic spindle and microtubule-motor protein interactions. Arrows depict the directional movement of the motor along the microtubule. (B) Schematic representation of stochastic microtubule states (left) and microtubule-motor protein interactions (right).

Figure S3: Centrosome movement and clustering is similar with 3, 4, 5, and 6 centrosomes. (A-C) Four centrosomes. Top: Trace of centrosome movement over time through the duration of a simulation. Bottom: Heat map representing the pairwise distances between all centrosome pairs indicated in the corresponding traces. From left to right, the case of enriched dynein in a region of $\pi/2$ in (A), uniform dynein in (B), and no dynein in (C). (D-F) Traces of five centrosomes for the case of enriched dynein in a region of $\pi/2$ in (D), uniform dynein in (E), and no dynein in (F). (G-I) Traces of six centrosomes for the case of enriched dynein in a region of $\pi/2$ in (G), uniform dynein in (H), and no dynein in (I). In the top panel of (A-C), along with panels (D-I), a red 'x' indicates initial centrosome position and a blue '*' indicates centrosome position at 30 minutes. Numbers mark individual centrosomes, grayscale indicates time, and pink on the cell boundary indicates the region of high dynein localization (where $P_{d_{cor}} = 0.5$; elsewhere $P_{d_{cor}} = 0.01$).

Figure S4: Computational models suggest centrosome clustering is sensitive to the size of the region of cortical dynein activity. (A-D) Top: Trace of centrosome movement over time through the duration of a simulation where a red 'x' indicates initial centrosome position, a blue '*' indicates centrosome position at 30 minutes. Numbers mark individual centrosomes, grayscale indicates time, and pink on the cell boundary indicates the region of high dynein activity (where $P_{d_{cor}} = 0.5$; elsewhere $P_{d_{cor}} = 0.01$). Dynein is enriched in a region of size $\pi/8$, $\pi/4$, $3\pi/4$, and π in panels A, B, C, and D, respectively. Bottom: Heat map representing the pairwise distances between all centrosome pairs indicated in the corresponding traces. (E) The percent of simulations with three or four centrosomes that achieve a bipolar spindle (each of the two poles with one or more clustered centrosomes) when cortical dynein activity is enriched in a region of size $\frac{\pi}{8}$, $\frac{\pi}{4}$, $\frac{\pi}{2}$ (3 centrosome condition represented in Figure 4 A,B), $\frac{3\pi}{4}$, and π.

Figure S5: Centrosome movement in computational simulations is driven by cortical dynein activity. (A,B) Plots depicting the magnitude of cortical dynein-derived forces over time (red bars, scale on left axis) and the distance between each centrosome and the midpoint of dynein enrichment (blue trace, scale on right axis) from the simulation with dynein enriched in the angular region from 0 to $\pi/2$ in A and uniform dynein in B (corresponding to simulations in Figure 4 B and D, respectively). (C) Distance between each centrosome and the region of dynein enrichment. (D) Distance between centrosome pairs. For simulations with uniform dynein, the distance is calculated as the minimum distance to the cell boundary. (E) Average number of peaks in cortical-dynein-derived force in simulations. In (C-E), noD, uD, and $(\pi/2)$D correspond to the cases of no dynein, uniformly distributed dynein, or dynein restricted to the angular region from 0 to $\pi/2$. Each dot represents a single centrosome's position (C), centrosome pair (D), or simulation (E). Quantification performed on 30 simulations from each condition. Significance determined by one-way ANOVA with Tukey's test for multiple comparisons; $*p < 0.05$, $****p < 0.0001$.

Figure S6: Computational modeling indicates that all motor and non-motor derived forces are dynamic over time. Plots depicting the magnitude of each force (scale on left axis) on each centrosome, and the corresponding centrosome position relative to the cell cortex (blue trace, scale on right axis) over time. Plots correspond to simulations as follows: (A) Figure 4 B, (B) Figure 4 D, and (C) Figure 4 E.

Figure S7: Asymmetric and dynamic cortical dynein localization aids centrosome clustering during computational modeling of spindle formation. A-C Top: Traces of centrosome movement over time from a simulation with enriched region of cortical dynein localization (with $P_{d_{cor}} = 0.5$) oscillating between the upper-right (solid pink arc, 0 to $\pi/2$) and lower-left quadrant (dashed pink arc, $-\pi$ to $-\pi/2$) of the cell with a period of $T = 1.67$ min (A) and $T = 2.33$ min (B). In (C), enrichment is only up to $T = 15$ min and then there is no dynein enrichment for $T \geq 15$ ($P_{d_{cor}} = 0.01$ everywhere on the cortex). Initial centrosome position indicated by a red 'x' and final centrosome position is indicated by a blue '*'. Color bar is time. A-C Bottom: Heat map representing the pairwise distances between all centrosome pairs from the simulation represented above. Black dotted lines indicate a timepoint when cortical dynein localization is redistributed. Color bar is distance. (D) Plots depicting the magnitude of cortical dynein-derived forces over time (red bars, scale on left axis) and the distance (blue traces, scale on right axis) between each centrosome and the midpoint of dynein localization from the simulation shown in (C).

Figure S8: Spindle length and dynein-derived forces are dynamic over time in cells with two centrosomes. (A) Traces of bipolar spindle length from 5 simulations with asymmetric dynein localization. (B) Traces of centrosome movement over time from a simulation with asymmetric dynein localization. Colorbar is time. (C) Plots depicting the magnitude of cortical dynein-derived forces (pink bars, scale on left axis) over time and the distance (blue trace, shown on right axis) between each centrosome and the midpoint of dynein localization from the simulation shown in (B).

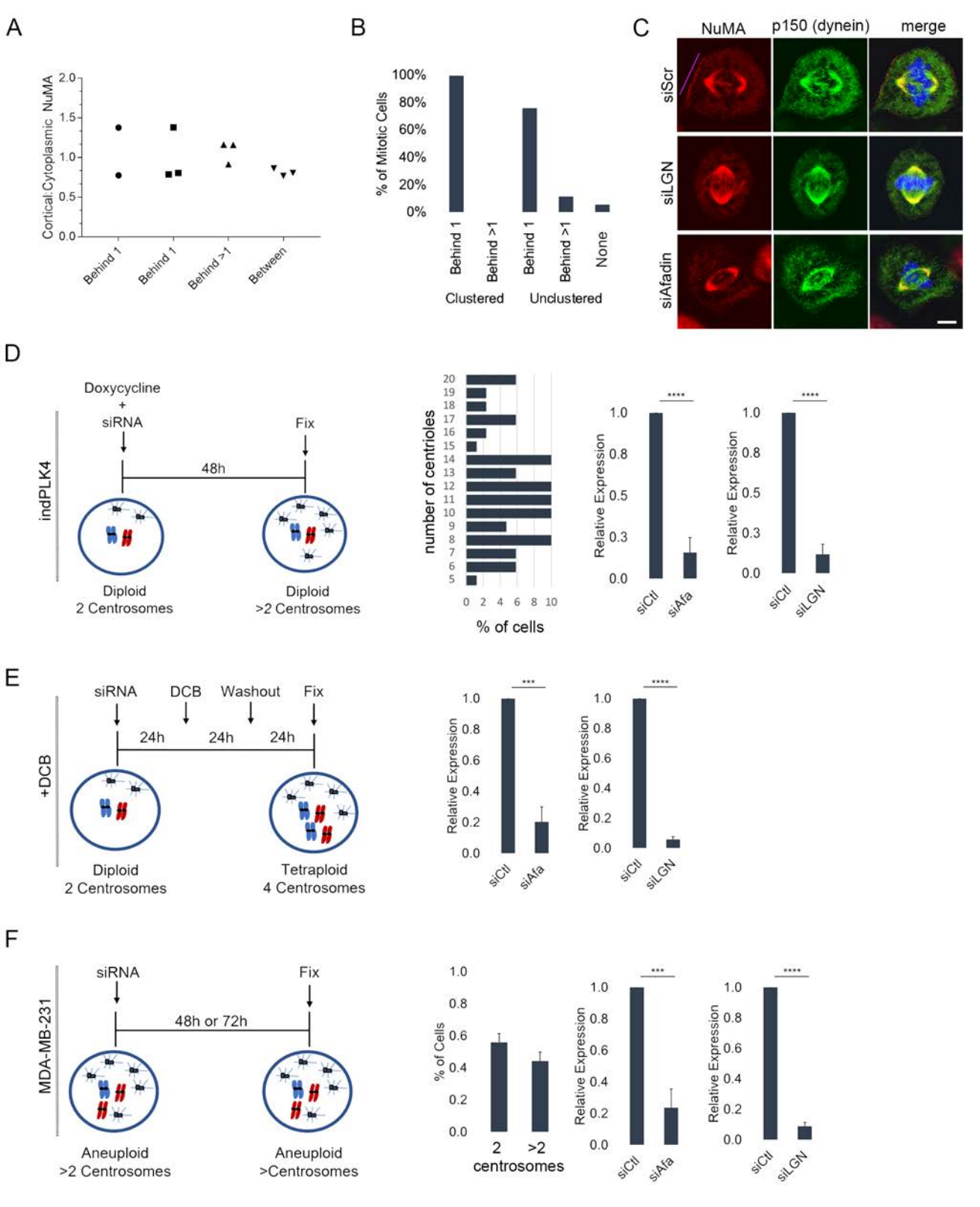
A
Cortical:Cytoplasmic NuMA
2.0
1.5
1.0
0.5
0.0
Behind 1
Behind 1
Behind >1
Between
B
% of Mitotic Cells
100%
80%
60%
40%
20%
0%
Behind 1
Behind >1
Behind 1
Behind >1
None
Clustered
Unclustered
C
NuMA
p150 (dynein)
merge
siScr
siLGN
siAfadin
D
indPLK4
Doxycycline
+
siRNA
Fix
48h
Diploid
2 Centrosomes
Diploid
>2 Centrosomes
number of centrioles
% of cells
Relative Expression
siCtl
siAfa
siLGN
****
E
+DCB
siRNA
DCB
Washout
Fix
24h
24h
24h
Diploid
2 Centrosomes
Tetraploid
4 Centrosomes
***
****
F
MDA-MB-231
siRNA
Fix
48h or 72h
Aneuploid
>2 Centrosomes
Aneuploid
>Centrosomes
% of Cells
2
>2
centrosomes

A

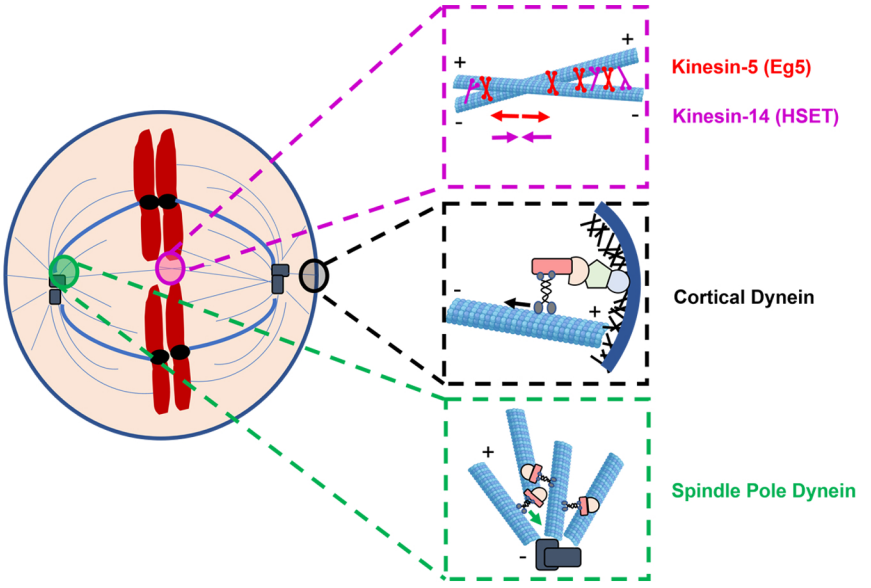
Kinesin-5 (Eg5)
Kinesin-14 (HSET)
Cortical Dynein
Spindle Pole Dynein

B

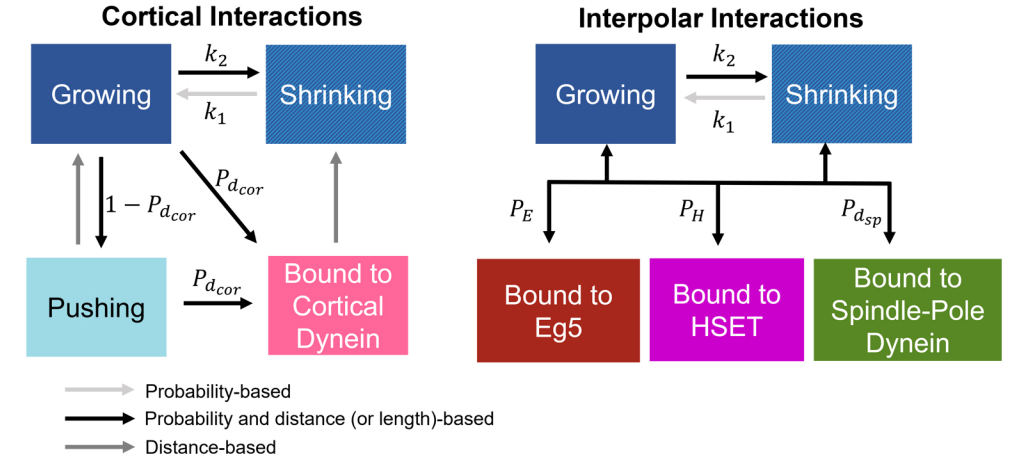
Cortical Interactions
Growing
Shrinking
k_2
k_1
$1 - P_{d_{cor}}$
$P_{d_{cor}}$
$P_{d_{cor}}$
Pushing
Bound to Cortical Dynein
Interpolar Interactions
Growing
Shrinking
k_2
k_1
P_E
P_H
$P_{d_{sp}}$
Bound to Eg5
Bound to HSET
Bound to Spindle-Pole Dynein
Probability-based
Probability and distance (or length)-based
Distance-based

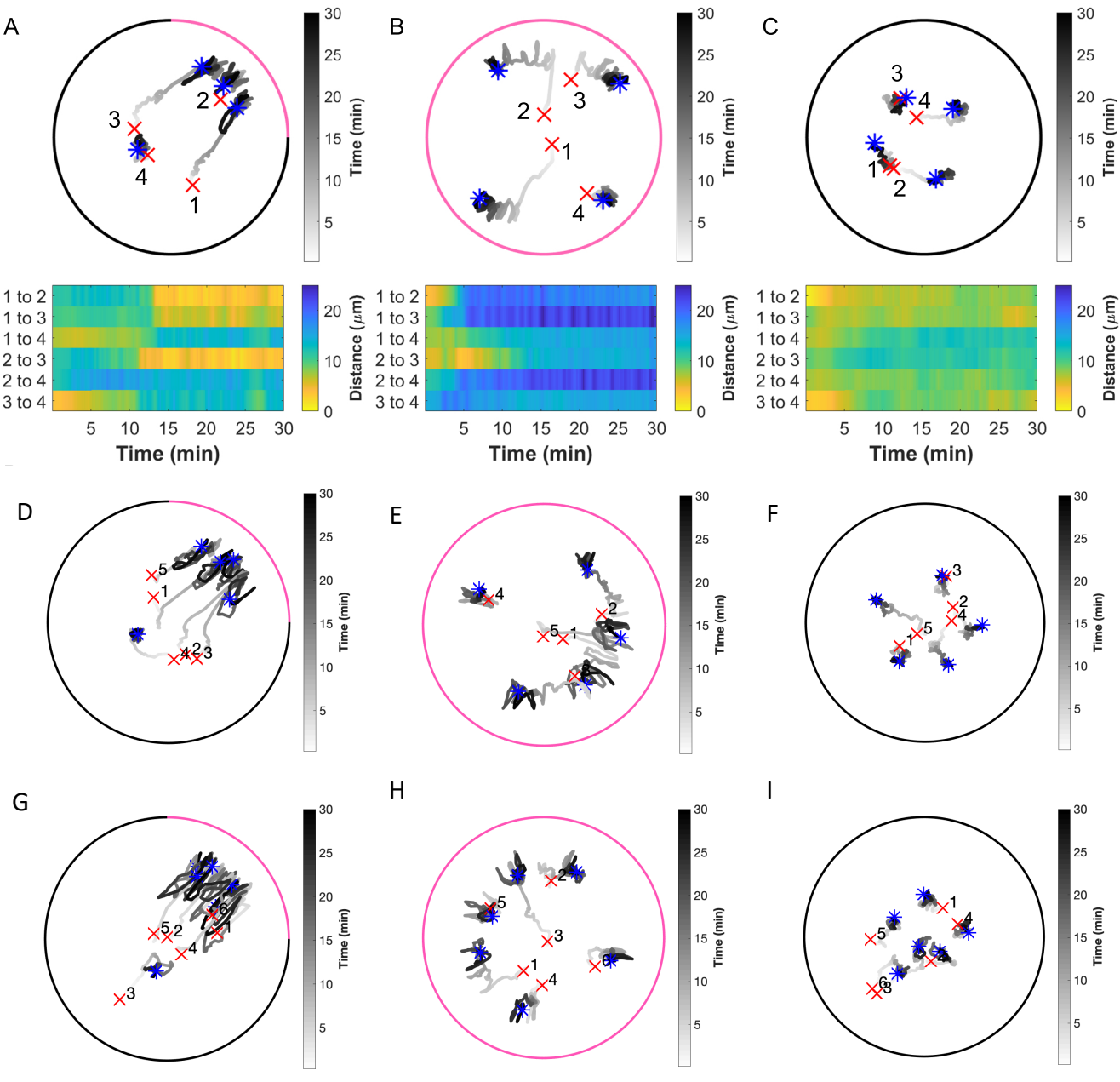
A
B
C
D
E
F
G
H
I
Time (min)
Distance (μm)
1 to 2
1 to 3
1 to 4
2 to 3
2 to 4
3 to 4
Time (min)

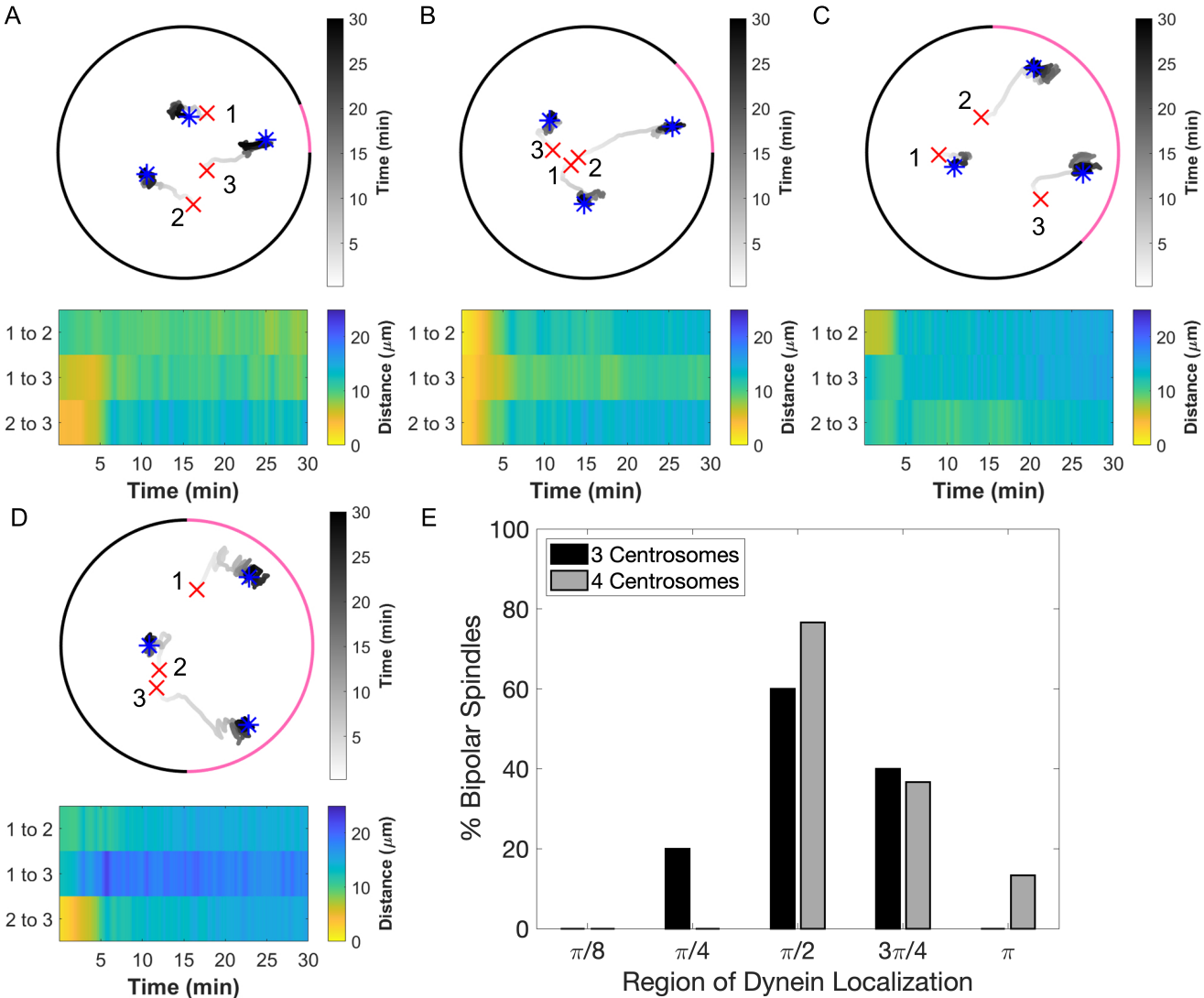
A
B
C
D
E
Time (min)
Distance (μm)
1 to 2
1 to 3
2 to 3
% Bipolar Spindles
3 Centrosomes
4 Centrosomes
π/8
π/4
π/2
3π/4
π
Region of Dynein Localization

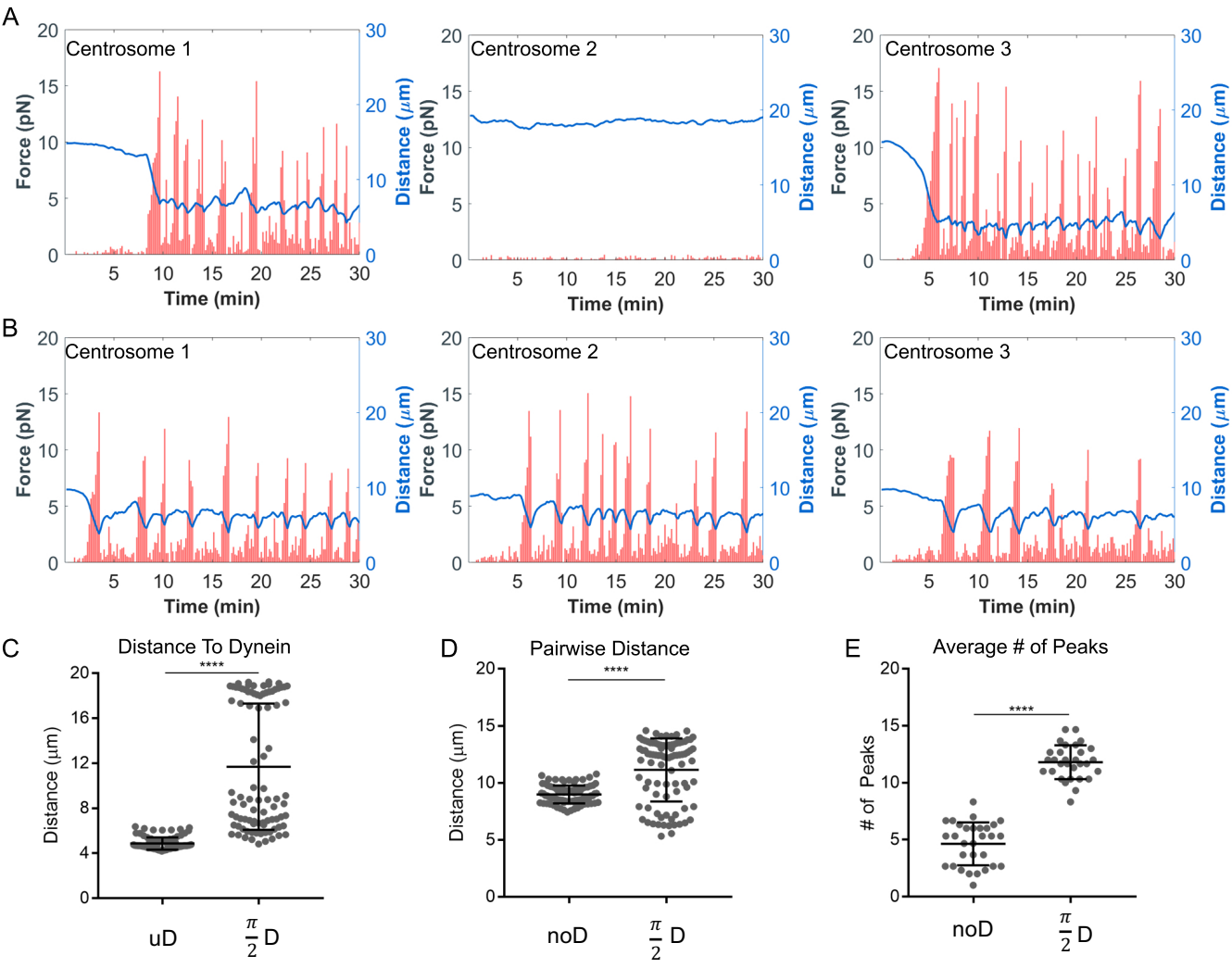
A
Centrosome 1
Centrosome 2
Centrosome 3
Force (pN)
Distance (μm)
Time (min)
B
Centrosome 1
Centrosome 2
Centrosome 3
Force (pN)
Distance (μm)
Time (min)
C
Distance To Dynein
****
Distance (μm)
uD
π/2 D
D
Pairwise Distance
****
Distance (μm)
noD
π/2 D
E
Average # of Peaks
****
# of Peaks
noD
π/2 D

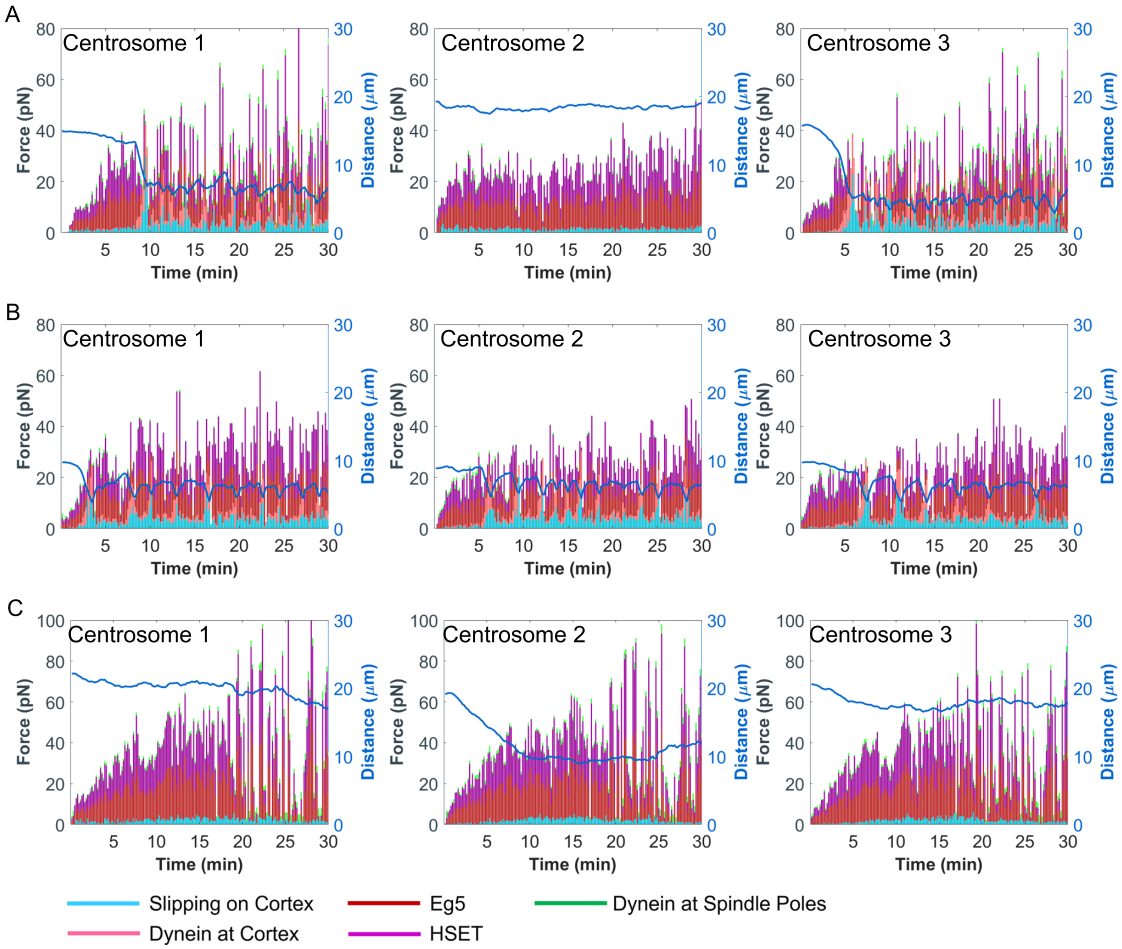

Figure S6: All motor and non-motor derived forces are dynamic over time. Plots depicting the magnitude of each force (scale on left axis) on each centrosome, and the corresponding centrosome position relative to the cell cortex (blue trace, scale on right axis) over time. Plots correspond to simulations as follows: (A) Figure 4B, (B) Figure 4D, and (C) Figure 4E.

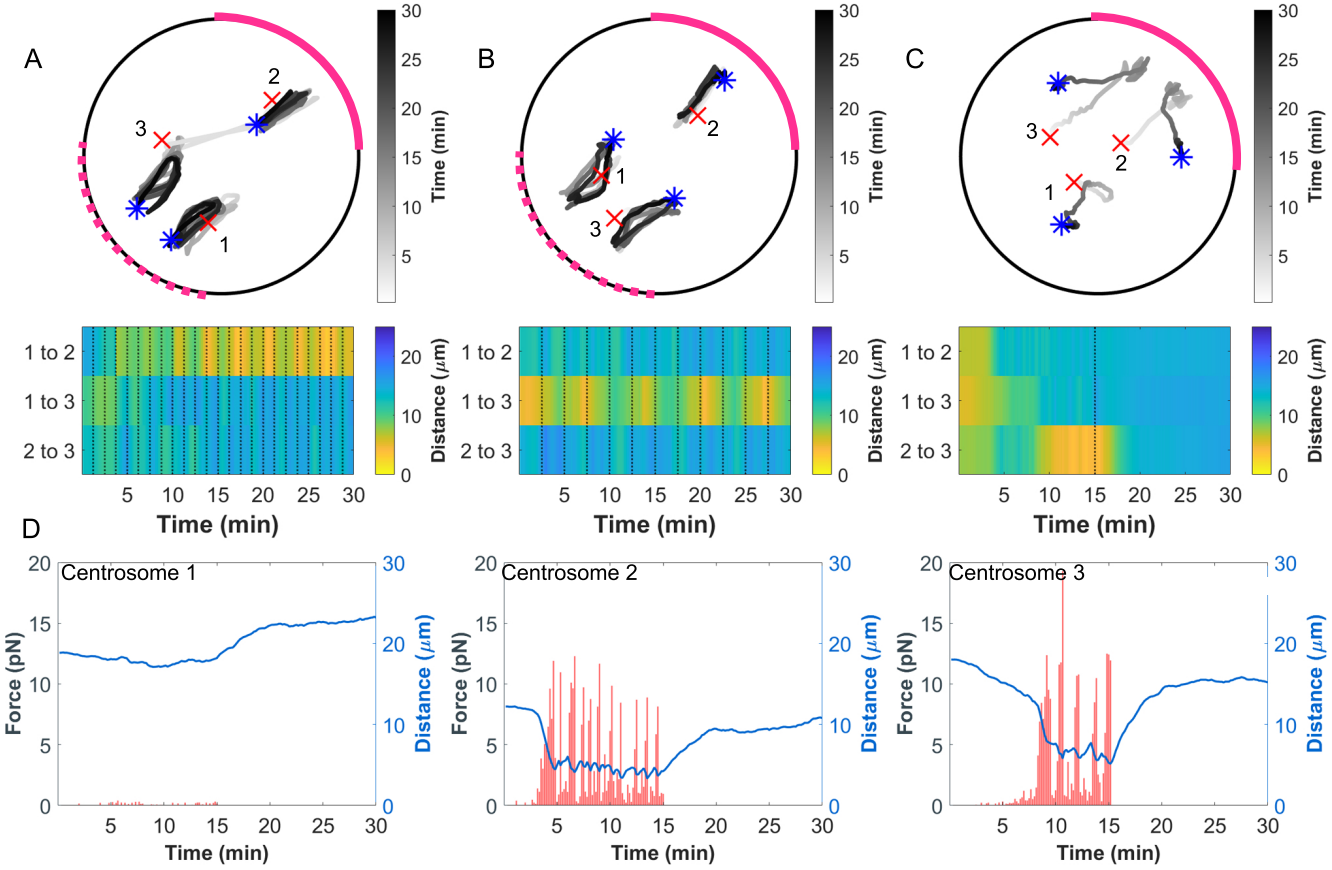
A
B
C
D
1
2
3
Time (min)
1 to 2
1 to 3
2 to 3
Distance (μm)
Time (min)
Centrosome 1
Centrosome 2
Centrosome 3
Force (pN)
Distance (μm)
Time (min)

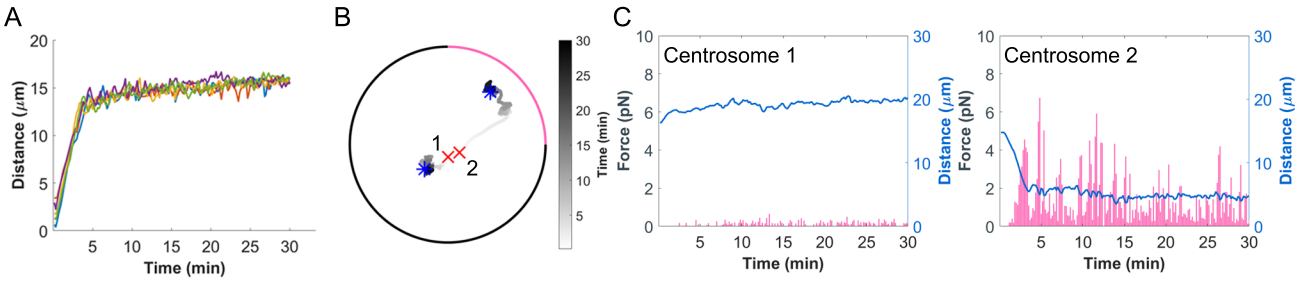
A
Distance (μm)
Time (min)
B
1
2
Time (min)
C
Centrosome 1
Force (pN)
Distance (μm)
Time (min)
Centrosome 2
Force (pN)
Distance (μm)
Time (min)

Table S1: Parameters. All parameter values without reference are approximated to match biological results.

Parameter	Value	Description	Reference
Microtubules			
v_g	0.183 μms^{-1}	Microtubule growth velocity (+ ends)	Piehl and Cassimeris (2003), Wu et al. (2011)
v_s	0.3 μms^{-1}	Microtubule shrinking velocity (+ ends)	Wu et al. (2011)
v_b	0.057 μms^{-1}	Microtubule shrinking velocity (+ ends) bound to cortical dynein	Laan et al. (2012)
k_1	0.167 s^{-1}	Rescue frequency	Wu et al. (2011), Komarova et al. (2002)
κ	10 pNμm^2	Bending rigidity	Laan et al. (2012), Li and Jiang (2017), Kikumotot et al. (2006)
f_{stall}	5 pN	Stall force of microtubules	Ma et al. (2013)
MT_{nuc}	2 s^{-1}	Microtubule nucleation rate per centrosome	Piehl et al. (2004)
θ	$10\pi/180$	Slipping microtubule angle change	
Motor Proteins			
Dynein			
$f_{0,d}$	3.6 pN	Stall force of dynein	Elshenawy et al. (2019)
$v_{0,d}$	0.86 μms^{-1}	Walking velocity of dynein	Urnavicius et al. (2018), Elshenawy et al. (2019)
$P_{d_{cor}}$	0.5	Probability of binding to cortical dynein	
$P_{d_{sp}}$	0.3	Probability of binding to spindle pole dynein	
$\mathcal{D}_{d_{cor}}$	$4v_g(dt)$ μm	Distance required for binding to cortical dynein	
$\mathcal{D}_{d_{sp}}$	1 μm	Distance required for binding to dynein at spindle poles	
Kinesin-5 (Eg5)			
$f_{0,Eg5}$	1.5 pN	Stall force of Eg5	Shimamoto et al. (2015)
$v_{0,Eg5}$	0.2 μms^{-1}	Walking velocity of Eg5	Li et al. (2019)
P_E	0.5	Probability of binding to Eg5	
Kinesin-14 (HSET)			
$f_{0,HSET}$	1.1 pN	Stall force of HSET	Roostalu et al. (2018)
$v_{0,HSET}$	0.2 μms^{-1}	Walking velocity of HSET	Li et al. (2019)
P_H	0.7	Probability of binding to HSET	
$\mathcal{D}_{Eg5,HSET}$	$v_g dt$ μm	Distance required for binding to Eg5 or HSET	
Other			
r	15 μm	Radius of the cell	
c_r	0.3 μm	Radius of a centrosome	
$\mathcal{D}_r$	2 μm	Distance for repulsive forces	
K	0.35	Microtubule length-dependent scaling factor	
C	0.01	Antiparallel crosslinking scaling factor	
s	0.075 μm^{-1}	Scaling for catastrophe frequency	
R	1 μm	Scaling for repulsive forces	
μ	0.7 pNsμm^{-2}	Viscosity of the cytoplasm	Luby-Phelps et al. (1993)
ξ	41.2 pNs	Drag coefficient	